Hierarchal Contribution of N- and C-Terminal Sequences to the Differential Localization of Homologous Sodium-Dependent Vitamin C Transporters, SVCT1 and SVCT2, in Epithelial Cells[†]

Saaket Varma,[‡] Kami Sobey,[§] Christine E. Campbell,[‡] and Shiu-Ming Kuo*[,‡,§]

Department of Biochemistry and Department of Exercise and Nutrition Sciences, University at Buffalo, Buffalo, New York 14214

Received December 16, 2008; Revised Manuscript Received February 10, 2009

ABSTRACT: Human sodium-dependent vitamin C transporters, SVCT1 and SVCT2, share 66% sequence identity yet localize in the apical and basolateral membranes of epithelial cells, respectively. This pair thus serves as a model for studying multipass membrane protein targeting. Domain swaps, deletions, insertions, and point mutations were performed on EGFP-tagged hSVCT1 and hSVCT2 plasmids. Mutant proteins stably expressed in MDCK cells were analyzed by confocal microscopy and Transwell ascorbate transport assays. These studies identified an SVCT2 basolateral targeting sequence (BTS) in the N-terminus, which is conserved among mammalian SVCT2 forms. The less conserved N-terminus of SVCT1 is not required for apical localization. The destruction of SVCT2 BTS led to apical localization of the protein in a manner independent of the C-terminal sequence. A C-terminal sequence present in both SVCTs appears to be required for plasma membrane incorporation and retention as its deletion led to an increased level of intracellular appearance of both apically and basolaterally targeted SVCTs in the absence or presence of BTS. Nevertheless, all C-terminal deletion mutants showed preferential apical transport activity, suggesting a greater importance of this sequence for basolateral targeting. Our results collectively suggested a default apical targeting of SVCT, which is consistent with the evolution-based prediction. The SVCT sorting model with a hierarchal contribution of N- and C-terminal sequences was compared to the observations made for other multipass membrane proteins. The involvement of both intracellularly localized termini of multipass membrane proteins in the sorting pathway suggests a more complex sorting mechanism compared to that for single-pass proteins.

Membrane proteins mediate the vital material and information exchange between cells and their environment. This exchange is more complex in polarized epithelial cells such as those that line the gastrointestinal tract and renal tubules because these cells face two different environments, the lumen and the plasma. As expected, distinct membrane protein distribution patterns are observed for apical and basolateral membranes. For the sodium-dependent transport of the reduced form of vitamin C (ascorbate), two functional proteins, SVCT1 and SVCT2, have been identified (*1*). They have nonredundant functions which is evident from knockout mouse studies (*2, 3*). Both transporters are expressed in the intestine and kidney (*4, 5*), two organs that need to transport vitamin C from lumen via the apical membrane as well as from blood circulation via the basolateral membrane. We found that exogenously expressed human SVCT1 and SVCT2 reside on the apical and basolateral membrane of intestinal and renal epithelial cells, respectively, despite their high degree of primary sequence homology (*5, 6*). Since the only variable in our system that can contribute to the differential localization of hSVCT1 and hSVCT2 is their peptide sequence, this pair of homologous proteins is an excellent model for mapping the sequences required for apical and basolateral targeting.

The sorting of membrane proteins in epithelial cells to apical and basolateral membranes has been studied for a variety of proteins, including secretory proteins, GPI-anchored proteins, proteins that traverse the lipid bilayer once (single-pass), and multipass membrane proteins (*7*−*10*). Because of their topological differences, sorting mechanisms may not be identical for these four groups of proteins. For example, while extracellular N-glycosylation is needed for proper apical sorting of single-pass proteins, it is not critical for apical protein secretion (*11*). The sorting of multipass transporter proteins like SVCT is believed to rely on intracellularly present sequences (*7*−*10*). However, while some publications ascribed importance for sorting to the N-terminus of their proteins of interest (*12*−*14*), others reported the importance of the C-terminus for a separate group of proteins (*15*−*22*). The alternative use of the N- or C-terminus for the sorting of different multipass membrane proteins suggests at least two different protein biogenesis pathways. The other possible explanation of this apparent inconsistency is that unlike the single-pass membrane proteins, maybe both terminal peptide signals are needed for the sorting of multipass proteins, or they may play two different roles in sorting: promoting plasma membrane

[†] This work was supported partly by the University at Buffalo Mark Diamond Research Fund (to S.V. and K.S.).

* To whom correspondence should be addressed. Telephone: (716) 829-3680. Fax: (716) 829-3700. E-mail: smkuo@buffalo.edu.

[‡] Department of Biochemistry.

[§] Department of Exercise and Nutrition Sciences.

10.1021/bi802294v CCC: $40.75
Published on Web 02/13/2009

incorporation and retention and specific targeting to apical or basolateral membrane. For hSVCT1,[1] the deletion or mutation of a segment of the C-terminal sequence led to a decrease in the level of apical membrane incorporation or retention of the protein but did not appear to increase its appearance in the basolateral membrane (*23*). To test the hypothesis that N- and C-termini act in tandem, we analyzed the contributions of both N- and C-termini of hSVCTs, and to examine their roles in plasma membrane incorporation and retention and specific membrane targeting separately.

To minimize ambiguities in data interpretation, we used MDCK cell lines stably expressing various mutants to avoid the potential effect of transfecting agents in transiently transfected cells (*24*). We performed live cell imaging on stably transfected cells to avoid the need for cell fixation and processing. Furthermore, cells from the same passage were used for the imaging studies and the measurement of ascorbate transport activity in Transwells. Transport activity measurements complement imaging for determining the protein integration into a specific membrane. To ensure that the EGFP-based confocal visualization captures full-length proteins, the EGFP tag was placed in the C-terminus after the SVCT sequence. Previously, we have shown that EGFP tagging does not affect the basic transport properties of hSVCT1 and hSVCT2 (*5, 6*).

EXPERIMENTAL PROCEDURES

Materials. L-[*carboxyl*-^{14}C]Ascorbic acid (13 mCi/mmol) was purchased from Amersham Biosciences (Buckingshire, England). L-Ascorbic acid (SigmaUltra) was from Sigma Aldrich (St. Louis, MO). All cell culture reagents were from Invitrogen Corp. (Carlsbad, CA), except characterized fetal bovine serum which was purchased from Hyclone, USA (Logan, UT). All other chemicals used were of reagent grade. Primers used for site-directed mutagenesis and for sequencing were from Operon Biotechnologies, Inc. (Huntsville, AL) (Table 1). The sequences of the parent EGFP-tagged proteins, hSVCT1-EGFP and hSVCT2-EGFP (*5*), are shown in Figure 1.

Plasmid Preparation and Generation of Stable Cell Lines Expressing SVCT Proteins. The QuikChange site-directed mutagenesis kit from Stratagene (La Jolla, CA) and The Phusion site-directed mutagenesis kit from New England Biolabs (Ipswich, MA) were used following the manufacturers' protocols to create mutant plasmids (Table 1). Domain swapping between hSVCT1 and hSVCT2 was achieved by first mutating hSVCT1 to generate single KpnI and PstI sites mimicking hSVCT2 (Figure 1). Restriction enzyme digestion of the resulting hSVCT1 and parental hSVCT2, gel purification, and ligation of the desired fragments were then performed to generate six chimeric constructs, 112, 122, 121, 211, 212, and 221. These constructs were named on the basis of the source (hSVCT1 or hSVCT2) of their N-terminus, TM1−10, and TM11−12 with the C-terminus. For example, SVCT112 would have the N-terminus of SVCT1, TM1−10 from SVCT1, and TM11−12 with the C-terminus from SVCT2. Constructs bearing point mutations were named using standard genetic nomenclature. The deletion mutants were named on the basis of the location of amino acid residues or TMs removed. The insertion mutants were named on the basis of the sequence inserted.

After transformation of chemically competent *Escherichia coli* (DH5α) and colony expansion, plasmids were purified using a Perfectprep Plasmid kit (Eppendorf, Hamburg, Germany) or a Zyppy Plasmid Miniprep kit (Zymo Research, www.zymoresearch.com). Mutant plasmids were sequenced using proper primers by the facility at Roswell Park Cancer Institute (Buffalo, NY) to confirm the accuracy of the intended mutations. Calcium phosphate-mediated transfection was used to introduce the mutant plasmids into MDCK cells (*5*). Stable transfectants were generated using G418 selection and maintained in the same high-glucose Dulbcco's modified Eagle's medium (Invitrogen) as the nontransfected MDCK cells but supplemented with 200 μg/mL G418 as described previously (*5*). To confirm the success of the transfection and the fidelity of the mutation, genomic DNA was extracted from the stable cell lines using a MasterPure DNA Purification Kit (Epicenter, Madison, WI) or following a published protocol (*25*) with a modification for 0.4×10^6 cells. The extracted DNA was subjected to PCR using appropriate primers to amplify the mutated region. PCR products of expected size were then gel purified (QIAquick gel extraction kit, Qiagen, Valendia, CA, or Zymoclean Gel DNA Recovery Kit, Zymo Research) and sequenced. All sequencing was performed by the facility at Roswell Park Cancer Institute. All experiments were performed on 12−17 day cultures of early passages of stable cell lines.

Uptake Assays and Data Analysis. Ascorbate uptake assays were performed on cells grown in six-well plates (for assessing accumulation through the apical membrane) or on Transwell permeable supports (Corning Inc., Corning, NY) (for assessing accumulation through the apical and basolateral membranes separately). Hanks' balanced salt solution (Invitrogen) supplemented with HEPES and penicillin-streptomycin was used as the transport buffer (*26*). Transport assays were carried out at 37 °C in a humidified chamber at pH 7 following our previously described protocol (*5, 26, 27*) using L-[*carboxyl*-^{14}C]ascorbic acid. The total protein content was determined by a modified Lowry assay with SDS using bovine serum albumin as the standard (*28*).

All transport activity measurements were conducted in triplicate wells, and the means and standard deviations of the three independent wells are shown. For experiments performed with triplicate Transwells, data are expressed as the percent distribution of activities between apical and basolateral membranes to circumvent the variation in expression efficiency that was observed among different mutants. In general, the plasmids bearing TM1−10 of hSVCT2 had a lower bacterial transformation and lower MDCK cell transfection efficiencies compared to those bearing TM1−10 of hSVCT1. Their level of protein expression was also reduced. As a result, these mutants exhibited lower confocal fluorescence signals and less sodium-dependent ascorbate transport activity.

Confocal Fluorescence Microscopy and Total Fluorescence Measurement. Postconfluent MDCK cells (12−17 days after seeding) used for imaging experiments were grown in the Lab-Tek II chambered cover glasses (Nalge Nunc

[1] Abbreviations: AsA, ascorbate; AQP, aquaporin; BTS, basolateral targeting sequence; hSVCT, human sodium-dependent vitamin C transporter; MDCK, Madin-Darby canine kidney; NaDC1, sodium-dependent dicarboxylate transporter 1; NBC-1, Na^+-HCO_3^- cotransporter 1; TM, transmembrane segment.

Table 1: Sequences of Forward Primers and Primer Pairs Used for the Mutagenesis of hSVCT

mutant	forward primer (5′ to 3′)[a]
Mutation on SVCT1 for Constructing Domain Swaps of hSVCT1 and hSVCT2	
PstI	GCTGTGGGGCTGTCTAACCTGCAGTTTGTGGACATGAAC
KpnI	GCTTCAGTGGGACCATCGCCGTGCCCTTCCTGC
hSVCT2 Deletion	
Δ1−12	CTACTCGTTTCTCTTACCAAATCAATGGAGGCTGGAAGTTCAACAG
Δ1−56	CTACTCGTTTCTCTTGAGGACACTGAGC
Δ14−30	CCACATCCAAATCAATGGCTTTCTTCACTCTTCC
Δ28−59	CAAATACGAAGACGAGGCATACACTACGGAAAACGG
Δ28−48	CAAATACGAAGACGAGGCACAGGACAATGAGGACACTGAG
Δ51−59	GCGGTGAGCAGGACTACACTACGGAAAACGG
Δ55−59	CGGTGAGCAGGACAATGAGGACACTTACACTACGGAAAACGG
Δ56−82	CAATGAGGACACTGAGGACCCCCAGCGAT
Δ617−634	AAAAAATACAGATGCTTCAAGAGCGACAACAGCCG
hSVCT2 Point Mutation[b]	
L56A	GAGGACACTGAGGCAATGGCGATCTACACTACGG
Y60A	GACACTGAACTCATGGCGATTGCGACTACGGAAAACGGCATT
L72A	GCAGAAAAGAGTTCCGCCGCTGAGACCCTGGATAGCACTGGC
L76A	GCAGAAAAGAGTTCCCTCGCTGAGACCGCCGATAGCACTGGC
L72A/L76A	GCAGAAAAGAGTTCCGCCGCTGAGACCGCCGATAGCACTGGC
L82A	GATAGCACTGGCAGCGCCGACCCCCAGCGATCAG
hSVCT1 Deletion[c]	
Δ2−14	GTGATTCCAAAGATGACCACCAGGGACCCC
Δ17−21	ATGAAACCACCCCGCTACCCACAGAG
Δ20−37	TACCAAGGTGGCACGGGGTCCCTGG
Δ1−30	TAGTGATTCCAAAGCCCACAGAGCCTAAGTTTT
Δ294−296	GCACGAACCGATGCCCGTATGGCTATTGC
Δ294−299	CGAACCGATGCCCGAGCACCCTGGAT
hSVCT1 Residues 294−299 Replaced with the Corresponding Sequence from hSVCT2	
Δ294−299QGVLLV[d]	CGAACCGATGCCCGTCAAGGCGTACTTCTGGTAGCACCCTGGAT
hSVCT1 N-Terminal Point Mutation[b]	
L32I	CTACCCACAGAGCCTAAGTTTGACATGATTTACAAGATAGAGGAC
Primer Pair for hSVCT2 Basolateral Targeting Sequence Insertion into hSVCT1 between Amino Acid Residues 31 and 32 (5′ to 3′)[e]	
Δ1−30+(50−64)	CTGATGGCGATTTACACCACCGAGAACATTTACAAGATAGAGGACGTGCC CTCGGTGTCCTCGTTGTCCATGTCAAACTTAGGCTCTGTGGG
Primer Pair for hSVCT1 TM Segment Deletion (5′ to 3′)[e, f]	
ΔTM3−12 (Δ100−519)	GAGCGTGGTCTGATACAGTGGAAAG GGTGGTCTGGATGAGAGTGGTGATG
ΔTM3−6 (Δ100−277)	CCCACAGACCCAAAAGCCTATGGC GGTGGTCTGGATGAGAGTGGTGATG
ΔTM7−12 (Δ286−519)	GAGCGTGGTCTGATACAGTGGAAAG GCCATAGGCTTTTGGGTCTGTGGG

[a] Except in those mutations that a different mutation strategy was used as described in footnote [e]. [b] Numbers indicate the amino acid residue that was mutated. Underlined letters represent nucleotide changes to achieve the desired mutation. [c] Numbers indicate the amino acid residues that were deleted. [d] QGVLLV are amino acid residues from hSVCT2 used to replace the corresponding hSVCT1 amino acid residues 294−299 (GDIMAI). [e] Pairs of primers were used to create the mutant following the manufacturor's protocol (NEB Phusion site-directed mutagenesis kit). [f] TM numbers represent the putative transmembrane segments (*29*) that were removed. Numbers in parentheses indicate the amino acid residues that were removed.

International, Naperville, IL) as described previously (*5*). Images were captured in the Confocal and 3-D Imaging Core Facility of the University at Buffalo. Because these analyses were carried out over a period of 3 years as different mutants were generated, some variations existed in the instrument parameters among different imaging sessions. Initially, a Nikon Diaphot fluorescence microscope was used as a part of the Bio-Rad MRC-1024 laser confocal microscope system. The confocal images were acquired within an enclosed 37 °C chamber with a Nikon 60× NA 1.4 objective. A 488 nm laser line for excitation was used with an emission band-pass filter of 522 ± 16 nm. In later experiments, a Zeiss LSM510 Meta system was used in conjunction with a Pecon 37 °C Heating Insert, a Zeiss 63× NA1.4 objective, a 488 nm excitation laser line, and a band-pass emission filter of 500−550 nm. Nikon images were processed with Velocity LE 2.6 (Improvision, Inc., Lexington, MA), and Zeiss images were processed with Velocity LE 2.6 or LE 3.7. To ensure that the microscope hardware and setting are not confounding factors in the observed protein localization, MDCK cells expressing wild-type hSVCT1-EGFP and hSVCT2-EGFP were analyzed in both confocal microscopes, and the results were the same.

To ensure a fair assessment, multiple confocal images were collected from different areas of the slide chamber for each cell line, and representative images are shown. Some slide chambers were subjected to a second session of imaging after a few additional days of growth to ensure that cells were fully differentiated. No adjustments of brightness, contrast, sharpness, etc., were made to any of the acquired images. Higher laser power was necessary to produce confocal images of some constructs with a lower level of fluorescence. As a result, a straight bright line at the basolateral side was observed due to the laser reflection from the glass coverslip (as a result of mismatch in the reflection index of the cell and the glass). For cell lines that lack a strongly defined apical or basolateral fluorescence, it is not possible to assign an apical or basolateral localization to the transfected protein

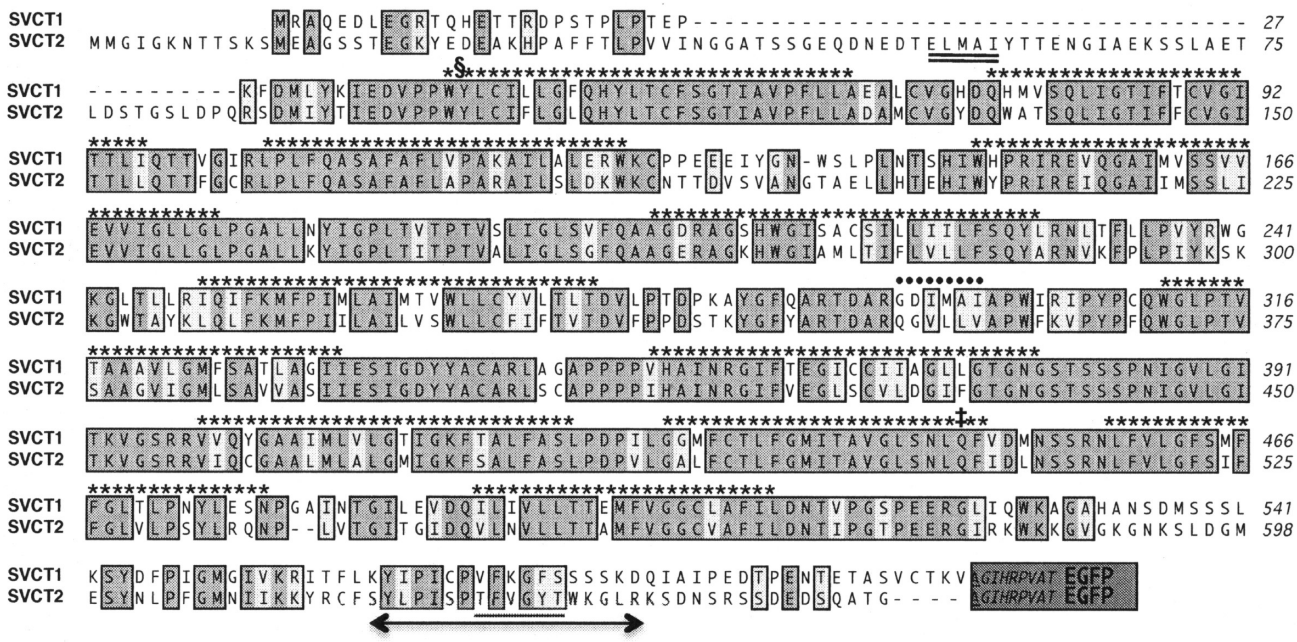

FIGURE 1: Protein alignment of hSVCT1-EGFP and hSVCT2-EGFP (*5*). Regions of homology are indicated with shades (dark gray for identical residues and light gray for conserved substitutions). Double-underlined sequence in the N-terminus indicates the minimum deletion we found that altered basolateral targeting (Figure 3B). The 12 predicted transmembrane segments (*29, 33*) are denoted with asterisks. The six hydrophobic amino acid residues that are examined in Figure 7A are denoted with circles. KpnI and PstI sites are indicated by § and ‡, respectively. Deletion of the arrowed sequence in SVCT2 disturbed plasma membrane incorporation and retention in our study (Figure 6). This sequence included the underlined region that was previously reported to be important for SVCT1 plasma membrane incorporation and retention (*23*).

by imaging alone since the imaging method does not provide information about the boundary of the cells. We tried to perform dye labeling to define the cellular boundary, but the inevitable emission spectrum overlap with EGFP along with the low level of EGFP fluorescence in such cell lines limited the application.

Total live-cell fluorescence emission from nontransfected MDCK cells and various lines of mutant-expressing MDCK cells grown in the 96-well plates was measured. A Biotek Synergy HT multi-detection microplate reader was used with excitation at 485 nm (slit width of 20 nm) and emission at 528 nm (slit width of 20 nm). Fluorescence was measured in the presence of Ca^{2+}- and Mg^{2+}-containing phosphate-buffered saline. Background fluorescence emission was also measured from wells with saline but no cells and subtracted from the sample measurement to obtain net fluorescence per well.

RESULTS

Domain Swapping Mutants of SVCT1 and SVCT2. To determine the importance of N- and C-termini of SVCTs individually, we made six domain-swapped SVCTs following a published topology prediction (*29*). The locations of the KpnI and PstI sites used for the construction of domain swapping mutants and the six constructs are shown in Figures 1 and 2A. N-Terminal swapping resulted in the exchange of only predicted N-termini, while C-terminal swapping resulted in the exchange of the predicted C-termini along with transmembrane segment (TM) 11−12. All chimeras were incorporated or retained in the cellular membrane as expected since the KpnI and PstI sites reside in regions that are conserved between SVCT1 and SVCT2 (Figure 1). The localization of chimeras as determined by confocal microscopy (Figure 2B) was consistent with the differential sodium-dependent ascorbate uptake in Transwells (Figure 2C). Nontransfected MDCK cells and MDCK cells expressing the parental SVCTs are included in Figure 2C for the sake of comparison. The three chimeras, 112, 122, and121 (Figure 2A), localized apically as shown in confocal images (Figure 2B) and also showed preferential transport from the apical membrane in the Transwell assay (Figure 2C). Conversely, the two basolaterally localized chimeras, 211 and 212, as seen in confocal images (Figure 2B), exhibited more uptake activity from the basolateral side similar to parental SVCT2 (Figure 2C). The remaining chimera, SVCT221, had a low level of expression that made unequivocal localization by confocal microscopy technically impossible. The emission from an individual confocal slice of SVCT221 was below the detection limit of confocal microscopy. However, the presence of the construct in the stably transfected cells was confirmed by DNA extraction of the stably transfected cells, PCR amplification of the mutated region, and the sequencing of the PCR band as described in Experimental Procedures. The linear response of the [^{14}C]ascorbate transport assay also allowed us to detect a preferential basolateral transport activity in MDCK cells (Figure 2C). In summary, on the basis of the results depicted in panels B and C of Figure 2, it appears that the N-terminal sequence dictates the polarized distribution of SVCT1 and SVCT2: constructs with the N-terminal sequence from SVCT1 show apical localization, while constructs with the N-terminal sequence from SVCT2 show basolateral localization. In contrast, the C-terminal sequences seem to be interchangeable between SVCT1 and SVCT2 with no effect on differential targeting to apical or basolateral membranes (Figure 2B,C).

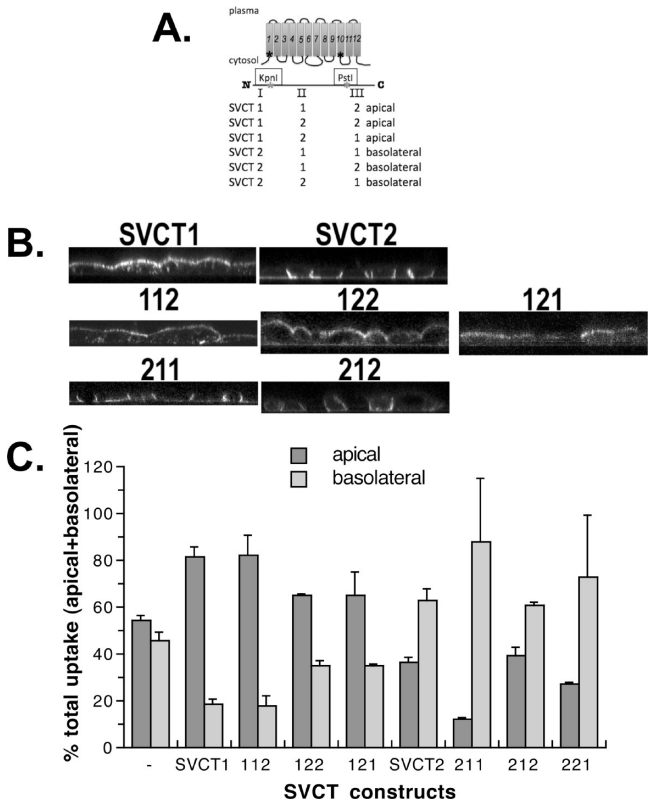

FIGURE 2: Effects of domain swapping between SVCT1 and SVCT2 on their polarized distribution in MDCK cells. (A) Predicted topology of SVCT (*29, 33*). Asterisks denote the KpnI site (at the start of the TM1) and the PstI site (at the end of TM10) used for swapping. The domain swapping mutants are named on the basis of the source of their segments I (N-terminus), II (TM1−10), and III (TM11−12 and C-terminus). For example, a mutant with segments I and II from SVCT1 and segment III from SVCT2 is named SVCT112. (B) Confocal images showing the apical localization of SVCT112, 122 and 121, and the basolateral localization of 211 and 212 in stably transfected MDCK cells. (C) Sodium-dependent ascorbate transport activities (at 10 μM ascorbate and 135 mM sodium) were measured in nontransfected MDCK cells (−) and MDCK cells stably transfected with various plasmids and grown on Transwells. Data shown are means ± the standard deviation of three independent Transwells and expressed as the relative activity distribution between apical and basolateral membranes (percent of total uptake). Some error bars are too small to be clearly visible. Results for SVCT1 and SVCT2 are from ref *6*.

N-Terminal Basolateral Targeting Sequence in SVCT2. One interpretation of our domain swapping data in Figure 2 is that a basolateral targeting sequence exists in the N-terminus of SVCT2, and thus, SVCT1 that normally resides in the apical membrane can be redirected to the basolateral membrane upon N-terminal swapping. To identify the putative basolateral targeting sequence in hSVCT2, two sets of N-terminal deletion plasmids were constructed. The first set of deletions removed residues up to E48. Basolateral localization of SVCTs was not affected by these deletions as observed by confocal imaging (Figure 3A). In Δ1−12 mutants, M13 could be an alternative translation starting site. In contrast, the second set of deletions removing further downstream residues led to a change in the localization from the basolateral membrane to the apical membrane as shown by confocal imaging (Figure 3B). The apically localized SVCTs that are expressed at high levels also exhibited particulate presence in the cytoplasm, which was reported previously for the parental SVCT1 (*5, 23*). The distribution of sodium-dependent vitamin C transport activity in MDCK cells stably expressing these mutants (Figure 3C,D) is consistent with the confocal observations. Mutations that did not affect the basolateral localization of the protein (Figure 3A) maintained a preferential uptake from the basolateral side of the Transwell (Figure 3C), while apically localized mutants (Figure 3B) acquired a preferential uptake from the apical side (Figure 3D). In two cases, matching mutations were performed on SVCT2 and SVCT211, SVCT2Δ1−12 and SVCT211Δ1−12 as well as SVCT2Δ1−12:Δ56−82 and SVCT211Δ1−12:Δ56−82 (Figure 3). Since both imaging and Transwell uptake results from these matching mutations in SVCT2 and SVCT211 are identical (Figure 3, first two mutants in panels A−D), and the level of expression of SVCT211 is higher than that of SVCT2, SVCT211 was used for most of the remainder of the N-terminal basolateral targeting signal studies.

Overall, deletions of SVCT2 N-terminus up to residue E48 did not affect the basolateral localization based on the confocal images and the transport activity measurement of deletion mutants (Figure 3A,C). The shortest deletion that can induce the basolateral to apical transition is the removal of amino acid residues 55−59 (ELMAI) (Figure 3B,D). In fact, the five mutations that led to the apical localization judged by the confocal imaging (Figure 3B) and the Transwell transport activity measurement (Figure 3D) all involved deletion of hydrophobic amino acid residues 56−59 (LMAI).

N-Terminal hydrophobic leucine and tyrosine residues have been reported to be important for the targeting of other multipass membrane proteins to the basolateral membrane (*12, 13*). Thus, as shown in Figure 4, we designed additional mutations to test the effect of mutating L56, which is within the minimum deletion resulting in apical localization (see above). The removal of the first 56 amino acids including Leu56 (Δ1−56) led to an increase in the degree of intracellular protein retention for both basolaterally localized SVCT2 and SVCT211 (Figure 4A, first two mutants). From the confocal images alone, we could not conclude whether the proteins were in the plasma membrane. Interestingly, preferential vitamin C transport activity at the apical membrane was observed for both Δ1−56 mutants (Figure 4B, first two mutants). Point mutation L56A similarly led to an increase in the level of intracellular localization of the protein (Figure 4A, third mutant), and transport activity was found in both the apical and basolateral membrane (Figure 4B, third mutant). In contrast, the Y60A mutation (immediately after LMAI) had no effect on the basolateral localization as determined by confocal imaging and Transwell uptake assay measuring sodium-dependent transport of vitamin C (Figure 4A,B, last mutant). Mutation of other further downstream N-terminal leucines (L72, L76, and L82) to alanine as shown in Figure 4C also had no effect on the basolateral localization as determined by confocal imaging.

Absence of the N-Terminal Apical Targeting Sequence in SVCT1. The apical localization of SVCT1 and SVCT122 (Figure 2) is consistent with the presence of apical targeting sequence in the N-terminus of SVCT1. However, we observed a transition from basolateral to apical localization when the basolateral target sequence within the SVCT2 N-terminus was destroyed without the addition of the SVCT1

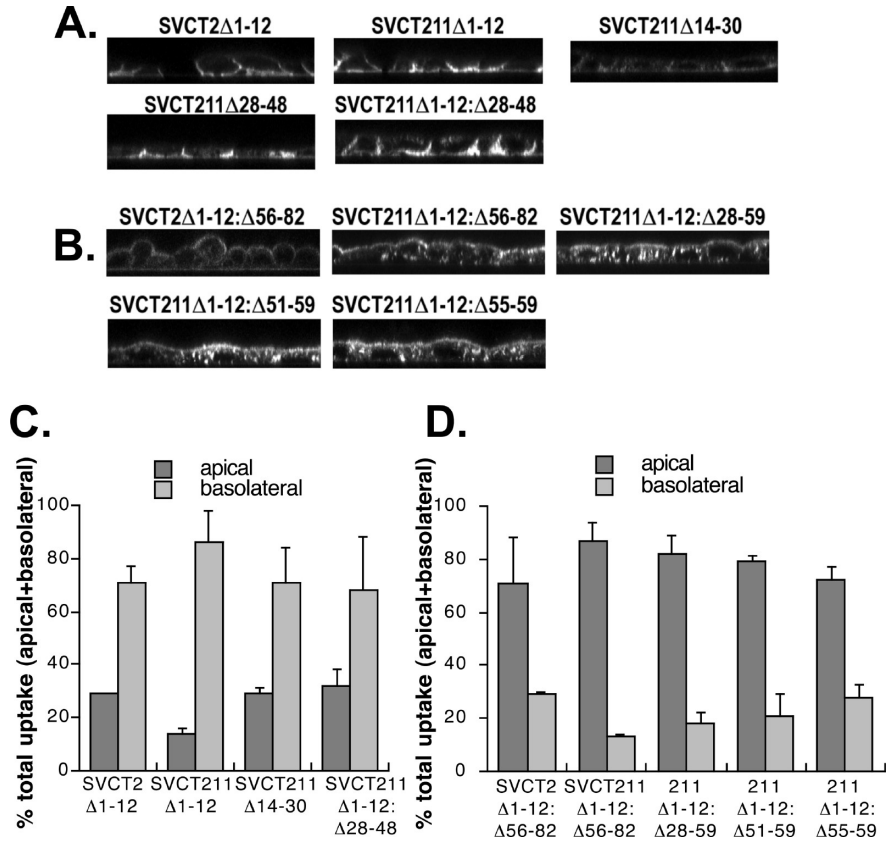

FIGURE 3: Effects of SVCT2 N-terminal deletions on the basolateral localization of SVCTs in stably transfected MDCK cells. (A) Confocal images of those SVCT2 N-terminal mutants that still have basolateral localization similar to that of SVCT2. (B) Confocal images of those SVCT2 N-terminal mutants that localize apically like SVCT1. (C and D) Sodium-dependent ascorbate transport activities (at 10 μM ascorbate and 135 mM sodium) were measured for mutant MDCK cells shown in panels A and B, respectively. Cells were grown on Transwells. Data shown are means ± the standard deviation of three independent Transwells and expressed as the relative activity distribution between apical and basolateral membranes (percent total uptake). Some error bars are too small to be clearly visible.

N-terminal sequence (Figures 3 and 4). These results suggest an alternative explanation; namely, apical localizations of SVCT1 and SVCT122 are simply consequences of the absence of an N-terminal basolateral targeting sequence rather than the presence of an N-terminal apical targeting sequence. To differentiate between these two possibilities, we prepared SVCT1 constructs with various N-terminal modifications to determine whether there is an apical targeting sequence in the N-terminus of SVCT1 (Figure 5).

Deleting up to 30 amino acids from the N-terminus of SVCT1 had no effect on apical localization as shown by confocal imaging (Figure 5A, first three mutants). The SVCT1Δ1−30 mutant which contained deletion up to the beginning of the extensive sequence homology between SVCT1 and SVCT2 (Figure 1) lost all SVCT1-specific N-terminal sequence. This mutant is presumed to use M31 as the translational start site. Although there was some difference in the sodium-dependent vitamin C transport activity among the three mutants, SVCT1Δ2−14, SVCT1Δ17−21, and SVCT1Δ1−30 (Figure 5B, first three mutants), it appears to be a consequence of a difference in protein expression. When the net monolayer EGFP fluorescence was plotted with the transport activity, fluorescence and uptake followed the same trends. Mutant SVCT1Δ2−14 had lower net EGFP fluorescence per well, and its sodium-dependent vitamin C transport activity was also lower. The fourth N-terminal deletion of SVCT1, SVCT1Δ20−37, removed six amino acid residues that are highly conserved between SVCT1 and SVCT2, ending three residues before the predicted starting site of TM1 (Figure 1). Although apical localization was still observed for this mutant by confocal imaging, the protein was also detected throughout the cell (Figure 5A, fourth mutant). In addition, a drastic loss of transport activity from the apical membrane relative to the net fluorescence per well was observed (Figure 5B, fourth mutant). In summary, the N-terminal SVCT1-specific sequence does not appear to contribute to apical targeting. Three unrelated multipass membrane proteins have also been shown to persistently localize in the apical membrane after the deletion of their N-terminal sequences (*12, 14, 30*), demonstrating that SVCT1 is not unique in this regard.

We then asked whether inserting N-terminal residues 50−64 of SVCT2 [which included residues 56−59 (LMAI) shown in Figure 3 to be necessary for the basolateral targeting] into SVCT1Δ1−30 immediately following the initiating methionine would direct SVCT1Δ1−30 to the basolateral membrane. Apical localization of SVCT1Δ1−30 was unaltered by the additional SVCT2 N-terminal residues 50−64 (Figure 5A, comparing the third and fifth mutant). Although there is a much lower sodium-dependent vitamin C transport activity across the apical membrane relative to its total fluorescence (Figure 5B, last mutant), a preference of transport across the apical membrane was confirmed in a separate Transwell transport assay (results not in the figure). Of the total Transwell sodium-dependent vitamin C transport activity of this mutant, 77 ± 9% was observed across the apical membrane with 23 ± 3% across the basolateral membrane. This transport activity distribution is similar to

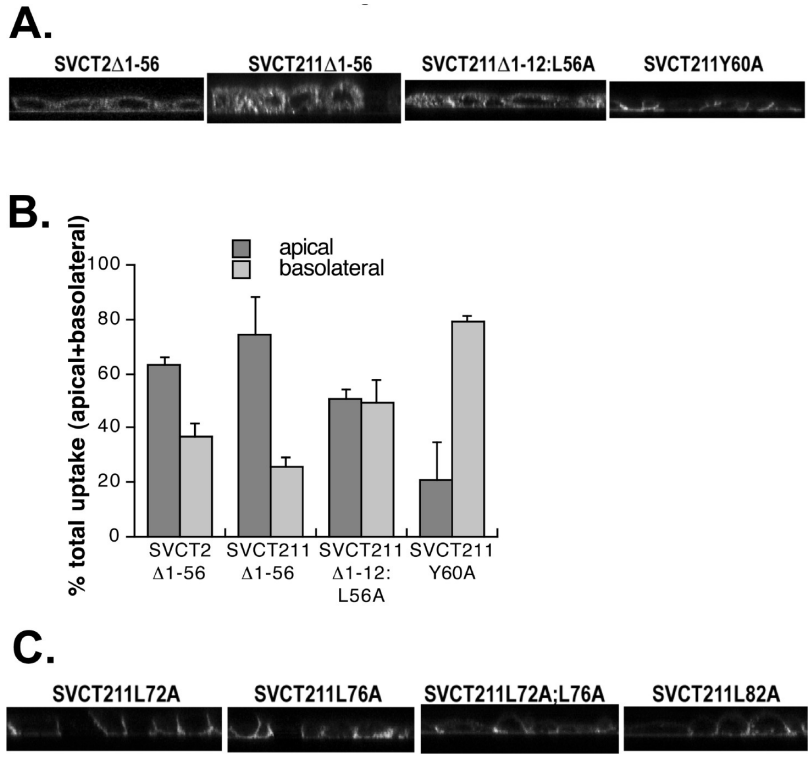

FIGURE 4: Comparison of SVCT2 N-terminal mutations that affect L56 to those that do not affect L56 on the basolateral localization of SVCTs in stably transfected MDCK cells. (A) Confocal images of SVCTs with a shortened N-terminal sequence of hSVCT2 (initiated at M57) with N-terminal point mutants. (B) Sodium-dependent ascorbate transport activities (at 10 μM ascorbate and 135 mM sodium) were measured for mutant MDCK cells shown in panel A. Cells were grown on Transwells. Data shown are means ± the standard deviation of three independent Transwells and expressed as the relative activity distribution between apical and basolateral membranes (percent total uptake). (C) Confocal images showing the localization of additional N-terminal point mutants of SVCT211 in stably transfected MDCK cells.

that of parental SVCT1 (Figure 2C). Thus, residues 56−59 of SVCT2 are necessary but likely not sufficient for basolateral targeting.

The C-Terminal Sequence Is Important for Plasma Membrane Localization. Since the result of domain swapping experiments (Figure 2) showed that the C-terminal sequences of SVCT1 and SVCT2 are interchangeable, the C-terminal sequence apparently does not determine differential targeting. However, our data did not rule out other functional roles for the C-terminus. Subramanian et al. (*23*) reported that a mutation in the C-terminus of SVCT1 led to a decrease in the level of membrane incorporation or retention of this protein. Interestingly, the C-terminal sequence that they examined is within a region of SVCT1 and SVCT2 homology (Figure 1). We hypothesized that rather than targeting, this C-terminal sequence may be important for proper plasma membrane incorporation or retention for both apical and basolateral membrane SVCT proteins. To test this hypothesis, we created a deletion mutation eliminating the C-terminal sequence of residues 617−634 of SVCT2 (Figure 1) targeting the corresponding homologous region that had been reported to be important for SVCT1 membrane incorporation or retention (*23*). The results of C-terminal deletion experiments are shown in Figure 6.

On the basis of the confocal images (Figure 6A), the deletion of residues in the C-terminus of the apically localized SVCT112 as well as the basolaterally localized SVCT2 and SVCT212 (Figure 2) all led to a decrease in the level of plasma membrane incorporation or retention. As described in Experimental Procedures, the transport assay and confocal imaging are both needed to determine the absence or presence of SVCTs in the plasma membrane. Transwell transport assays of these three C-terminal deletion mutations revealed sodium-dependent vitamin C transport activities. For all three mutants, transport activity was higher in the apical membrane than in the basolateral membrane (Figure 6B). In summary, the C-terminal sequence is important for proper apical and basolateral localization of SVCTs, serving to ensure proper plasma membrane incorporation and retention. The preferential activity distribution of all C-terminal deletion mutants to the apical membrane implies that the N-terminal basolateral targeting sequence cannot function properly in the absence of the C-terminal sequence.

Analysis of the Transmembrane Domain of SVCT1. Our results in Figures 2, 5, and 6 failed to identify an N- or C-terminal apical targeting sequence unique to SVCT1. If apical targeting is sequence-guided, the sequence in question must then reside within the transmembrane domain. To locate such a sequence, we performed mutation of the transmembrane domain of SVCT1. The first set of mutations, as shown in Figure 7A, targeted the GDIMAI sequence between putative TM6 and TM7 (Figure 1). The predicted intracellular localization of this sequence and a difference between SVCT1 and SVCT2 in this region make this sequence a possible candidate for apical targeting. Removing the first three amino acids, GDI, from SVCT112 did not affect the apical localization based on the results of confocal imaging (Figure 7A, left). Removing all six amino acids, GDIMAI, led to a loss of defined membrane localization, apical or basolateral, based on confocal imaging (Figure 7A, middle). A conformation change resulting from the removal of a string

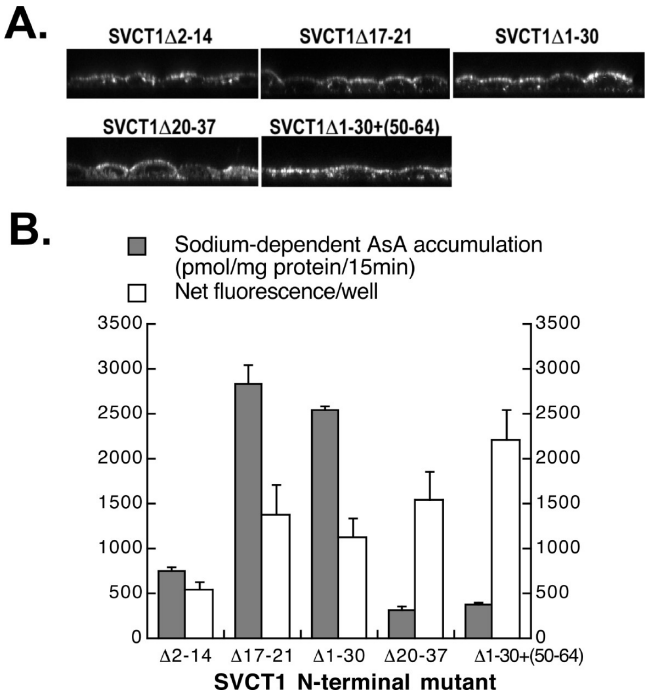

FIGURE 5: Effects of N-terminal deletions of SVCT1 and subsequent insertion of SVCT2 N-terminal residues 50−64 on the apical localization of SVCT1 in stably transfected MDCK cells. (A) Confocal images showing the localization of N-terminal mutants of SVCT1. SVCT1Δ1−30+(50−64) was derived from SVCT1Δ1−30 and contains SVCT2 N-terminal residues 50−64 inserted after the starting M31. (B) Transport activities (at 10 μM ascorbate and 135 mM sodium) were measured for cells grown in the six-well plates. The net live-cell monolayer fluorescence per well was obtained by subtracting the no-cell background fluorescence from the total monolayer fluorescence of each cell line grown on a 96-well plate. Data shown are means ± the standard deviation of three independent wells for the transport activity and four independent wells for the fluorescence. (-) Nontransfected MDCK cells.

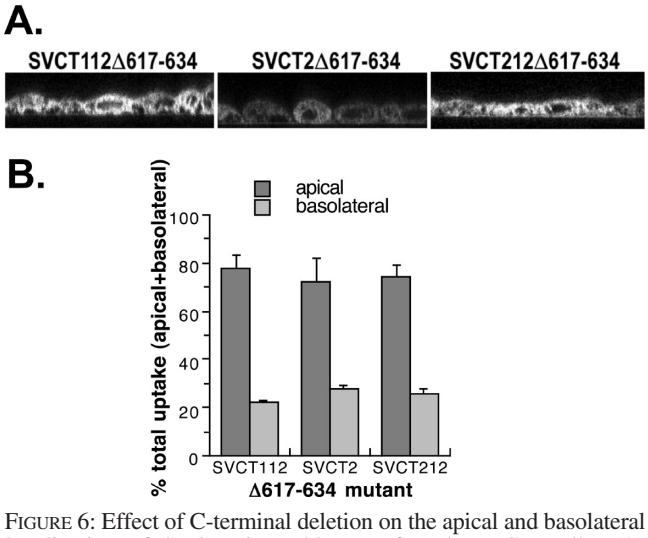

FIGURE 6: Effect of C-terminal deletion on the apical and basolateral localization of SVCTs in stably transfected MDCK cells. (A) Confocal images showing the protein localization of three SVCT constructs with 18 amino acids deleted (Δ617−634) from the C-terminal SVCT2 sequence. (B) Transport activities (at 10 μM ascorbate and 135 mM sodium) were measured in Transwells for MDCK cells and various mutants containing SVCT2 C-terminal deletions. Data shown are means ± the standard deviation of three independent Transwells and expressed as the relative activity distribution between apical and basolateral membranes (percent total uptake). (-) Nontransfected MDCK cells (same as shown in Figure 2C).

of six amino acids most likely accounted for the observed distribution pattern of SVCT112Δ294−299, as replacing the six amino acids with that from the SVCT2, QGVLLV, led to the restoration of apical localization (Figure 7A, right). Since the mutant with SVCT2 sequence, QGVLLV, localized in the apical membrane, this predominantly hydrophobic GDIMAI sequence of SVCT1 is unlikely to be important for apical targeting. This observation is consistent with the apical localization that we observed for SVCT122 (Figure 2B,C).

Another approach that we took to determine the importance of the transmembrane domain to the apical targeting was to perform TM deletion of SVCT1. Following the predicted TM junctions (*29*), we constructed three mutants with even numbers of TMs deleted, SVCT1ΔTM3−12, SVCT1ΔTM3−6, and SVCT1ΔTM7−12. The even-number deletion of TMs is to preserve the overall topology of the remaining protein. All three mutants exhibited little or no plasma membrane-localized fluorescence. The confocal images of two mutants, SVCT1ΔTM3−12 and SVCT1ΔTM3−6, are shown in Figure 7B. Interestingly, despite a lack of membrane-localized fluorescence, the total monolayer fluorescence of these two mutants (Figure 7C) was similar to the fluorescence that was observed for N-terminal deletion mutants of SVCT1 (Figure 5B). Thus, the TM deletion mutants are likely expressed. Protein conformation changes due to the extensive deletion most likely disturbed the process of plasma membrane incorporation and retention. TM deletion-associated loss of membrane localization has also been reported for the cystic fibrosis transmembrane regulator and thiamine transporter 1 (*31, 32*).

DISCUSSION

In this study, stably transfected mutants of EGFP-tagged SVCTs were used to determine the functional significance of N- and C-terminal sequences in the differential sorting of SVCTs in polarized epithelial cells. We identified an N-terminal basolateral targeting sequence, the absence of an N-terminal apical targeting sequence, and demonstrated the importance of the C-terminal sequence for both apical and basolateral membrane incorporation and retention. In addition, our results, when compared to observations made on other multipass membrane proteins, suggest a reconciliation of some seemingly contradictory conclusions on differential sorting in epithelial cells. Furthermore, our data provided limited information about the TM arrangement and functional domains of SVCT.

Using multiple mutations, and two complementary analysis methods (confocal imaging and Transwell transport activity measurements), we identified a basolateral targeting sequence in the N-terminus of basolaterally localized SVCT2 in stably transfected MDCK cells (Figures 2−4). When the entire N-terminus of SVCT2 (99 residues) was used to replace the N-terminus of SVCT1, the proteins, SVCT211 and -212, were redirected to the basolateral membrane (Figure 2). Deletion mutation up to amino acid residue 48 of the N-terminus of SVCT2 did not affect their basolateral localization (Figure 3A,C). Residues 56−59 (LMAI) seem to be the most critical part of the basolateral targeting sequence as all deletion mutations that removed these four residues led to the redirecting of the basolateral membrane

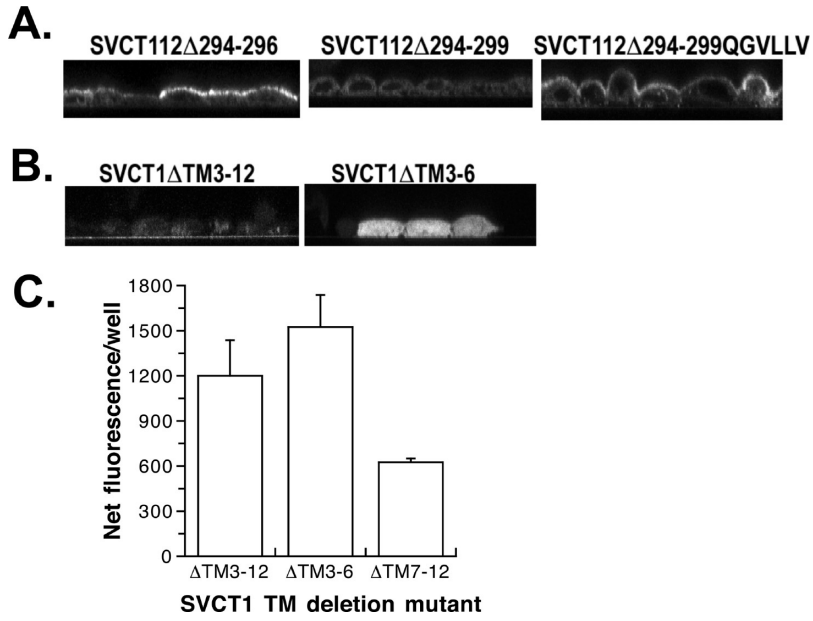

FIGURE 7: Effect of mutation in the transmembrane domain of SVCT1 on localization of the protein in stably transfected MDCK cells. (A) Confocal images of SVCT112 mutants with three amino acids (294−296) and six amino acids (294−299) removed from the predicted (*29*) intracellular loop between TM6 and TM7, or with the six amino acids (294−299) replaced by the corresponding sequence from SVCT2. (B) Confocal images of SVCT1 mutants with deletion of TM3−12 and TM3−6. (C) Net fluorescence from cells stably transfected with TM deletion mutants grown on 96-well plates. The net fluorescene per well shown was calculated by subtracting the background value obtained in the absence of cells from the total fluorescence of each cell line grown on the 96-well plate. Data shown are means ± the standard deviation of four independent wells. (-) Nontransfected MDCK cells.

protein to the apical membrane (Figure 3B,D). L56, although more important than Y60, L72, L76, and L82 in basolateral targeting (Figure 4), is only a part of this critical hydrophobic motif as point mutation L56A did not lead to the same preferential apical transport activity as the Δ55−59 mutant (Figure 4B compared to Figure 3D).

The four amino acid residues in the N-terminus of SVCT2, residues 56−59 (LMAI), although necessary for basolateral targeting, do not appear to be sufficient to redirect other multipass membrane proteins to the basolateral membrane. In fact, inserting amino acid residues 50−64 from the N-terminus of SVCT2 into an SVCT1 construct, SVCT1Δ1−30, that was devoid of all SVCT1-specific N-terminal sequence failed to redirect SVCT1Δ1−30 to the basolateral membrane [Figure 5, last mutant SVCT1Δ1−30+(50−64)]. Since SVCT211Δ14−30 and SVCT211Δ1−12:Δ28−48 localize in the basolateral membrane (Figure 3A,C), SVCT2 N-terminal residues up to E48 most likely do not contribute to the conformation of basolateral targeting sequence. The sufficient basolateral targeting sequence has to be from SVCT2 N-terminal residue 49 to TM1. Another observation that supports the essential but not sufficient nature of LMAI on basolateral targeting is that a virtually identical sequence (IMAI) is present in the predicted intracellular-facing TM6 and -7 junction of the apically localized SVCT1 (Figure 1).

The importance of hSVCT2 N-terminal residues in basolateral targeting is consistent with the complete cross-species conservation of this region in mammals and would suggest that SVCT2 may be basolaterally localized in epithelial cells of other species. As expected, SVCT2 was found to localize in the basolateral membrane of mouse small intestinal epithelial cells on the basis of our immunofluorescence studies of frozen sections (S.-M. Kuo, unpublished observations).

Using deletion mutation and a combination of confocal imaging and ascorbate transport assay, we found that N-terminal deletion of up to the first 30 residues had no effect on the apical localization of SVCT1 (Figure 5, mutants 1−3). It is important to note that the homology between hSVCT1 and hSVCT2 starts at D30 of SVCT1 (Figure 1). Thus, the Δ1−30 deletion has removed all SVCT1-specific sequence in the N-terminus. This lack of N-terminal apical targeting sequence does not contradict the results of our domain swapping experiments in Figure 2. The apical localization of SVCT122 and 121 can easily be rationalized by the removal of the N-terminal basolateral targeting sequence discussed above. Unlike SVCT2, the N-terminus of SVCT1 has a lower degree of cross-species conservation. Our conclusion that apical localization of hSVCT1 does not depend on a specific N-terminal sequence would predict that SVCT1 in other species with N-terminal sequences different from that of human could also be apically localized. The observed renal vitamin C reabsorption defect in SVCT1-knockout mice (*2*) supports this prediction, but the prediction has yet to be tested for nonmammalian species.

On the basis of the localization of chimeras (Figure 2), C-terminal sequences of SVCT1 and SVCT2 clearly could not have the targeting function that we demonstrated for the N-terminus of SVCT2. The confocal image and Transwell transport activity measurement (*5*) (Figure 2) consistently showed that SVCT1 and SVCT121, -112, and -122 are all in the apical membrane while SVCT2 and SVCT212 and -211 are in the basolateral membrane. However, the C-terminus could be important in other aspects of protein trafficking. Our results on the importance of the C-terminus (Figure 6) complement the observation previously made for SVCT1. There, deleting or mutating a segment of the SVCT1 C-terminal sequence led to an increase in the level of

intracellular retention but not basolateral membrane localization of SVCT1 (*23*). In Figure 6A, removing a similar segment from the SVCT2 C-terminus (Δ617−634) also led to an increase in the level of intracellar retention of SVCT2. Using the domain swapping mutants that we created as the template, we further demonstrated the importance of this C-terminal SVCT2 sequence in the plasma membrane incorporation or retention of other apically and basolaterally localized SVCTs (SVCT112Δ617−634 and SVCT212Δ617−634, respectively) (Figure 6A).

The exact role of the C-terminal sequence is likely to be more complex. The Transwell transport activity measurement (Figure 6B) reveals that C-terminal deletion mutants of originally apically and basolaterally localized SVCTs all ended up with more transport activity from the apical membrane than from the basolateral membrane. The observation suggests that the C-terminal sequence, although it does not possess an apical or basolateral membrane targeting function, is more important for promoting the incorporation and retention into the basolateral membrane than into the apical membrane. We note that the putative SVCTs in distantly related species such as *Caenorhabditis elegans* or *Drosophila melanogaster* have C-terminal sequences at least partially conserved [Y(I/L)P(I/L/F)XP] versus what we and Subramanian et al. (*23*) have examined.

With the apparent absence of an apical targeting sequence in the N- or C-terminus of SVCT1 (Figures 2 and 5), our logical next question is whether there could be apical targeting sequence in the transmembrane domain. Several lines of observations suggest that if such apical targeting sequence exists, it is within transmembrane domain sequences common to SVCT1 and SVCT2. SVCT1, -112, -122, and -121, with the transmembrane domain from SVCT1 or SVCT2, are all in the apical membrane (Figure 2). An SVCT2 N-terminal mutant was localized in the apical membrane in the absence of any SVCT1-specific sequence (Figure 3, SVCT2Δ1−12:Δ56−82). The apical localization of SVCT122 and -121 (using the transmembrane domain of SVCT2) also suggests that an interaction between the SVCT1-specific transmembrane domain sequence and apical membrane phospholipid is not critical for apical targeting. In fact, the ability of SVCT1 to move to the basolateral membrane after acquiring an intracellular N-terminal basolateral targeting sequence from SVCT2 (became SVCT211) (Figure 2) and then move back to the apical membrane when the basolateral targeting sequence was destroyed (such as hSVCT211Δ1−12:Δ55−59 in Figure 3) precludes any significant role of specific lipid−protein interaction in the specific membrane targeting of SVCTs. Our data do not dispute the importance of lipid environment in membrane protein incorporation and retention. Although N-glycosylation has been shown to be important for the apical targeting of a single-pass membrane protein (*11*), the putative SVCT1-specific N-glycosylation sites (*33, 34*) were absent in SVCT122, yet SVCT122 is properly localized in the apical membrane (Figure 2). In addition, SVCTs moved to the apical membrane whenever the basolateral targeting sequence was destroyed (Figure 3). Even the C-terminal mutants that had disturbed plasma membrane incorporation and retention exhibited more transport activity in the apical membrane (Figure 6). Overall, a lack of targeting function of SVCT1-specific sequence implies that even if an apical targeting sequence exists, it may not be separable from the sequence that is required for proper plasma membrane incorporation and retention. This conclusion is consistent with the evolution-based default apical localization prediction (*24*). In a single-cell organism, the entire plasma membrane faced the environment and is thus all apical membrane, whereas basolateral membranes came into existence only with the development of multicellular animals.

After the model for SVCT has been built, it is useful to consider whether the model fits with the observations made for other multipass membrane proteins. In our model, N-terminal sequence plays a role for basolateral targeting (Figures 3 and 4) but not for apical targeting (Figure 5) while C-terminal sequence plays a general role in plasma membrane incorporation and retention and is a prerequisite for basolateral targeting (Figure 6). Several observations made on other multipass membrane proteins are consistent with this model. The aquaporin (AQP) family represents the only other multipass membrane protein family in which both N- and C-termini have been examined. The N-terminal sequence of basolaterally localized AQP-3 can redirect apical AQP-2 to the basolateral membrane (*13*). N-Terminal deletion of AQP-5 did not affect its apical localization, but its C-terminal deletion mutant lost plasma membrane incorporation and retention (*30*). Some other multipass proteins have been studied for the importance of one of the termini, although for the most part, no information is available on the Transwell differential transport activity. Deletion of C-terminal sequence of apically localized sodium-dependent bile acid transporter or excitatory amino acid transporter 3 led to a diffused protein distribution pattern (*15, 18*) similar to that shown in Figure 6 and by Subramanian et al. (*23*). Also, removing N-terminal sequences of sodium-dependent dicarboxylate transporter 1 (NaDC1) and dopamine transporter did not affect their apical localization (*12, 14*). These observations made on apical transporters, similar to the SVCT1 observation, are consistent with the prediction of an evolution-based default apical localization hypothesis (*24*).

For basolateral transporters, in addition to SVCT2 and AQP-3 described above, the N-terminal sequence of NaDC3 is also important for its basolateral localization and can redirect NaDC1 to the basolateral membrane (*14*). The N-terminal sequence of the basolateral norepinephrine transporter can direct its family member, apical dopamine transporter, to the basolateral membrane (*12*). C-Terminal deletion of basolateral Na^+-HCO_3^- cotransporter 1 (NBC-1) led to a distribution throughout the cells similar to our confocal image in Figure 6 (*19, 35*). The N-terminus of NBC-1 was not examined. C-Terminal dileucine motifs were proposed to serve as the basolateral targeting sequence for sulfate anion transporter 1 and Na-K-Cl transporter 1 (*16, 21*), but again the N-termini of these proteins were not examined.

Interestingly, all basolateral targeting sequences reported contain hydrophobic residues (*12*−*14*) such as the four critical amino acid residues, LMAI, we found for SVCT2 (Figure 3). Hydrophobic amino acids are frequently involved in three-dimensional protein−protein interaction (*36*). The expected interaction between the basolateral targeting motif and the cellular protein sorting machinery would predict that an amino acid sequence of considerable length for the formation of a unique conformation (*36*) will be needed for basolateral targeting. This may explain our observation in

Figure 5 where a 15-amino acid insertion shortly upstream of TM1, although containing LMAI critical for basolateral targeting, failed to direct SVCT1 to the basolateral membrane. Also, because of the large size of the interface, single or multiple alanine mutations around the critical residues may not be enough to destroy the binding (*36*). This may explain our results of several point mutants such as L56A, Y60A, L72A, L76A, and L82A (Figure 4A−C).

Our mutation analysis of SVCTs also provided information in validating the predicted topology and structure−function relationship of SVCTs. We have shown that TM1 is critical for the function of SVCT1 (*6*). The predicted start of TM1 is in the vicinity of W41 (*29*), and the prediction is likely reasonable. N-Terminal deletion up to D30 of SVCT1 had no effect on the apical localization or transport activity, but a deletion of amino acids 20−37 of SVCT1 led to a drastic decrease in the transport activity relative to its total fluorescence along with more intracellular retention (Figure 5). Also, compared to the N-terminally truncated SVCT1 (SVCT1Δ1−30), the N-terminal insertion mutant SVCT1Δ1−30+(SVCT2 50−64) showed low transport activity relative to its total fluorescence (Figure 5B). It is possible that the loss of activity in the last two mutants reflects a perturbance in the structure around TM1.

The deletion and replacement of SVCT1 residues 294−299 (GDIMAI) shown in Figure 7A represents an anaylsis of the transmembrane domain. This region is clearly not in the middle of any TM as the removal of the first three amino acids had no effect on the apical localization (Figure 7A, left). The removal of all six amino acids may have disturbed protein folding since a loss of membrane localization was observed. The replacement with six amino acids from SVCT2 (QGVLLV) restored apical localization.

Of the limited set of mutants that we examined for sodium-independent vitamin C transport or dehydroascorbate transport activity, we did not observe any increase above the level of the wild-type MDCK cells, suggesting that none of the mutations altered substrate selectivity. Preliminary kinetic measurement indicates that the SVCT112 chimera containing the first 10 TMs (of a total 12 TMs) from SVCT1 has a K_m close to that of hSVCT1 (78 μM) while the equally apically localized chimera SVCT122 containing the first 10 TMs of SVCT2 has a lower K_m similar to the lower K_m observed for hSVCT2 (*5*). This suggests that differences in transport kinetics between hSVCT1 and hSVCT2 map to the first 10 TMs of the protein and is consistent with our previous publication demonstrating that TM1 contributes to the substrate binding of SVCT1 (*6*).

In summary, utilizing a mutation approach coupled with stable construct expression, live-cell imaging, and Transwell functional assays, we have identified the signals contributing to the differential sorting of two homologous proteins, hSVCT1 and hSVCT2. A major contribution of our work is to point out the necessity of examining both N- and C-termini of each multipass membrane protein for their roles in protein sorting and to separate the two aspects of sorting: incorporation and retention in the plasma membrane and targeting to a specific membrane. In this case, we conclude that the N-terminus of SVCT2 contains the basolateral targeting sequence while the C-terminal sequences of both SVCT1 and SVCT2 are important for the incorporation and retention in the plasma membrane. In addition, the C-terminal sequence is also needed to allow basolateral targeting as the N-terminal basolateral targeting sequence cannot function properly in the absence of the C-terminal sequence. No SVCT1-specific apical targeting sequence is found, and results from various experiments support a default presence of SVCT1 in the apical membrane of polarized MDCK cells, consistent with the evolution-based prediction. Our model of a separate presence of targeting sequence and plasma membrane incorporation and retention sequence in two intracellularly localized termini will contribute to the understanding of differential sorting of other multipass membrane proteins in epithelial cells.

ACKNOWLEDGMENT

We appreciate the technical guidance of Dr. Wade Sigurdson, Director of Confocal and 3-D Imaging Facility of the University at Buffalo. In-depth discussions with Dr. Murray J. Ettinger of the Department of Biochemistry, University at Buffalo, and his insight in protein chemistry contributed to the interpretation of the data.

REFERENCES

1. Takanaga, H., MacKenzie, B., and Hediger, M. A. (2004) Sodium-dependent ascorbic acid transporter family SLC23. *Pfluegers Arch. 447*, 677–682.
2. Corpe, C., Tu, H., Wang, J., Eck, P., Wang, Y., Schnermann, J., Faulhaber-Walter, R., Nussbaum, R., and Levine, M. (2007) SVCT1 (Slc23a1) knockout mice: Slc23a1 as the vitamin C kidney reabsorptive transporter. *FASEB J. 21*, lb520.
3. Sotiriou, S., Gispert, S., Cheng, J., Wang, Y., Chen, A., Hoogstraten-Miller, S., Miller, G. F., Kwon, O., Levine, M., Guttentag, S. H., and Nussbaum, R. L. (2002) Ascorbic acid transporter Slc23a1 is essential for vitamin C transport into the brain and for perinatal survival. *Nat. Med. 8*, 514–517.
4. Kuo, S. M., MacLean, M. E., McCormick, K., and Wilson, J. X. (2004) Gender and sodium-ascorbate transporter isoforms determine ascorbate concentrations in mice. *J. Nutr. 134*, 2216–2221.
5. Boyer, J. C., Campbell, C. E., Sigurdson, W. J., and Kuo, S.-M. (2005) Polarized localization of vitamin C transporters, SVCT1 and SVCT2, in epithelial cells. *Biochem. Biophys. Res. Commun. 334*, 150–156.
6. Varma, S., Campbell, C., and Kuo, S. (2008) Functional role of conserved transmembrane segment 1 residues in human sodium-dependent vitamin C transporters. *Biochemistry 47*, 2952–2960.
7. Muth, T., and Caplan, M. (2003) Transport protein trafficking in polarized cells. *Annu. Rev. Cell Dev. Biol. 19*, 333–366.
8. Rodriguez-Boulan, E., Kreitzer, G., and Musch, A. (2005) Organization of vesicular trafficking in epithelia. *Nat. Rev. Mol. Cell Biol. 6*, 233–247.
9. Ellis, M., Potter, B., Cresawn, K., and Weisz, O. (2006) Polarized biosynthetic traffic in renal epithelial cells: Sorting, sorting, everywhere. *Am. J. Physiol. 291*, F707–F713.
10. Fölsch, H. (2008) Regulation of membrane trafficking in polarized epithelial cells. *Curr. Opin. Cell Biol. 20*, 208–213.
11. Potter, B., Ihrke, G., Bruns, J., Weixel, K., and Weisz, O. (2004) Specific N-glycans direct apical delivery of transmembrane, but not soluble or glycosylphosphatidylinositol-anchored forms of endolyn in Madin-Darby canine kidney cells. *Mol. Biol. Cell 15*, 1407–1416.
12. Gu, H., Wu, X., Giros, B., Caron, M., Caplan, M., and Rudnick, G. (2001) The NH_2-terminus of norepinephrine transporter contains a basolateral localization signal for epithelial cells. *Mol. Biol. Cell 12*, 3797–3807.
13. Rai, T., Sasaki, S., and Uchida, S. (2006) Polarized trafficking of the aquaporin-3 water channel is mediated by an NH2-terminal sorting signal. *Am. J. Physiol. 290*, C298–C304.
14. Bai, X., Chen, X., Feng, Z., Hou, K., Zhang, P., Fu, B., and Shi, S. (2006) Identification of basolateral membrane targeting signal of human sodium-dependent dicarboxylate transporter 3. *J. Cell. Physiol. 206*, 821–830.
15. Cheng, C., Glover, G., Banker, G., and Amara, S. G. (2002) A novel sorting motif in the glutamate transporter excitatory amino

acid transporter 3 directs its targeting in Madin-Darby canine kidney cells and hippocampal neurons. *J. Neurosci. 22*, 10643–10652.
16. Regeer, R. R., and Markovich, D. (2004) A dileucine motif targets the sulfate anion transporter sat-1 to the basolateral membrane in renal cell line. *Am. J. Physiol. 287*, C365–C372.
17. Deen, P., Van Balkom, B., Savelkoul, P., Kamsteeg, E., Van Raak, M., Jennings, M., Muth, T., Rajendran, V., and Caplan, M. (2002) Aquaporin-2: COOH terminus is necessary but not sufficient for routing to the apical membrane. *Am. J. Physiol. 282*, F330–F340.
18. Sun, A. Q., Salkar, R., Sachchidanand, Xu, S., Zeng, L., Zhou, M. M., and Suchy, F. J. (2003) A 14-amino acid sequence with a β-turn structure is required for apical membrane sorting of the rat ileal bile acid transporter. *J. Biol. Chem. 278*, 4000–4009.
19. Li, H. C., Worrell, R. T., Matthews, J. B., Husseinzadeh, H., Neumeier, L., Petrovic, S., Conforti, L., and Soleimani, M. (2004) Identification of a carboxyl-terminal motif essential for the targeting of Na^+-HCO_3^- cotransporter NBC1 to the basolateral membrane. *J. Biol. Chem. 279*, 43190–43197.
20. Bedoukian, M. A., Whitesell, J. D., Peterson, E. J., Clay, C. M., and Partin, K. M. (2008) The stargazin C terminus encodes an intrinsic and transferable membrane sorting signal. *J. Biol. Chem. 283*, 1597–1600.
21. Carmosino, M., Giménez, I., Caplan, M., and Forbush, B. (2008) Exon loss accounts for differential sorting of Na-K-Cl cotransporters in polarized epithelial cells. *Mol. Biol. Cell 19*, 4341–4351.
22. Klapper, M., Daniel, H., and Döring, F. (2006) Cytosolic COOH terminus of the peptide transporter PEPT2 is involved in apical membrane localization of the protein. *Am. J. Physiol. 290*, C472–C483.
23. Subramanian, V. S., Marchant, J. S., Boulware, M. J., and Said, H. M. (2004) A carboxy-terminal region dictates the apical plasma membrane targeting of the human sodium-dependent vitamin C transporter-1 in polarized epithelia. *J. Biol. Chem. 279*, 27719–27728.
24. Mostov, K., Apodaca, G., Aroeti, B., and Okamoto, C. (1992) Plasma membrane protein sorting in polarized epithelial cells. *J. Cell Biol. 116*, 577–583.
25. Wang, Z., and Storm, D. R. (2006) Extraction of DNA from mouse tails. *BioTechniques 41*, 410–412.
26. Kuo, S.-M., Morehouse, H. F. J., and Lin, C.-P. (1997) Effect of antiproliferative flavonoids on ascorbic acid accumulation in human colon adenocarcinoma cells. *Cancer Lett. 116*, 131–137.
27. Kuo, S.-M., and Lin, C. P. (1998) 17β-Estradiol inhibition of ascorbic acid accumulation in human intestinal Caco-2 cells. *Eur. J. Pharmacol. 361*, 253–259.
28. Peterson, G. L. (1983) Determination of total protein. *Methods Enzymol. 91*, 95–119.
29. Liang, W. J., Johnson, D., and Jarvis, S. M. (2001) Vitamin C transport systems of mammalian cells. *Mol. Membr. Biol. 18*, 87–95.
30. Wellner, R., Hong, S., Cotrim, A., Swaim, W., and Baum, B. (2005) Modifying the NH2 and COOH termini of aquaporin-5: Effects on localization in polarized epithelial cells. *Tissue Eng. 11*, 1449–1458.
31. Subramanian, V. S., Marchant, J. S., Parker, I., and Said, H. M. (2003) Cell biology of the human thiamine transporter-1 (hTHTR1). Intracellular trafficking and membrane targeting mechanisms. *J. Biol. Chem. 278*, 3976–3984.
32. Cebotaru, L., Vij, N., Ciobanu, I., Wright, J., Flotte, T., and Guggino, W. (2008) Cystic fibrosis transmembrane regulator missing the first four transmembrane segments increases wild type and ΔF508 processing. *J. Biol. Chem. 283*, 21926–21933.
33. Tsukaguchi, H., Tokui, T., Mackenzie, B., Berger, U. V., Chen, X. Z., Wang, Y., Brubaker, R. F., and Hediger, M. A. (1999) A family of mammalian Na^+-dependent L-ascorbic acid transporters. *Nature 399*, 70–75.
34. Subramanian, V. S., Marchant, J. S., Reidling, J. C., and Said, H. M. (2008) N-Glycosylation is required for Na^+-dependent vitamin C transporter functionality. *Biochem. Biophys. Res. Commun. 374*, 123–127.
35. Espiritu, D. J., Bernardo, A. A., and Arruda, J. A. (2006) Role of NH_2 and COOH termini in targeting, stability, and activity of sodium bicarbonate cotransporter 1. *Am. J. Physiol. 291*, F588–F596.
36. Bogan, A., and Thorn, K. (1998) Anatomy of hot spots in protein interfaces. *J. Mol. Biol. 280*, 1–9.

BI802294V